Published in final edited form as:
Nano Lett. 2008 November ; 8(11): 3715–3723. doi:10.1021/nl801958b.

Nanocrystal core high-density lipoproteins: A multimodality contrast agent platform

David P. Cormode[1], **Torjus Skajaa**[1,2], **Matti M. van Schooneveld**[3], **Rolf Koole**[3], **Peter Jarzyna**[1], **Mark E. Lobatto**[1], **Claudia Calcagno**[1], **Alessandra Barazza**[1,3], **Ronald E. Gordon**[5], **Pat Zanzonico**[6], **Edward A. Fisher**[4], **Zahi A. Fayad**[1,*], and **Willem J. M. Mulder**[1,*]

[1] *Translational and Molecular Imaging Institute, Mount Sinai School of Medicine, One Gustave L. Levy Place, Box 1234, New York, NY 10029, Tel: 212-241-6858, Fax: 240-368-8096, Zahi.Fayad@mssm.edu, Willem.Mulder@mountsinai.org* [2] *Faculty of Health Sciences, Århus University, Vennelyst Boulevard 9, 8000 Århus C, Denmark* [3] *Condensed Matter and Interfaces, Debye Institute, Utrecht University, Princetonplein 5, 3584 CC Utrecht, The Netherlands* [4] *Department of Medicine (Cardiology), Marc and Ruti Bell Vascular Biology and Disease Program and the NYU Center for the Prevention of Cardiovascular Disease, New York University School of Medicine, New York University, Smilow 8 522 First Ave., New York, NY 10016* [5] *Department of Pathology, Mount Sinai Hospital, One Gustave L. Levy Place, New York, New York 10029* [6] *Departments of Medical Physics and Radiology, Memorial Sloan-Kettering Cancer Center, 1275 York Avenue, New York, NY 10021*

Abstract

High density lipoprotein (HDL), is an important natural nanoparticle that may be modified for biomedical imaging purposes. Here we developed a novel technique to create unique multimodality HDL mimicking nanoparticles by inclusion of gold, iron oxide or quantum dot nanocrystals for computed tomography, magnetic resonance and fluorescence imaging, respectively. By including additional labels in the corona of the particles, they were made multi-functional. The characterization of these nanoparticles, as well as their *in vitro* and *in vivo* behavior revealed that they closely mimic native HDL.

Inorganic nanocrystals such as gold particles, iron oxides or quantum dots can be used as contrast agents for medical imaging.[1] The high X-ray attenuation of gold nanoparticles is useful for contrast in computed tomography (CT)[2] and their optical properties have been exploited for a variety of imaging techniques.[3] Iron oxides have been widely used to produce contrast for magnetic resonance imaging (MRI) purposes, including targeted molecular imaging and cell tracking.[4–7] Quantum dots have unique fluorescence properties, such as a narrow and well-defined emission peak, are not prone to photobleaching and have therefore been demonstrated to be very valuable for fluorescence-based imaging.[8–10]

The study of natural nano-sized particles such as viruses, ferritin and lipoproteins is now contributing significantly to nanotechnology.[11,12] These natural nanoparticles may be modified for nanomedicinal purposes. For example, high density lipoprotein (HDL) is composed of a hydrophobic core of triglycerides and cholesterol esters covered in a monolayer of phospholipids, into which apolipoprotein A-I (apoA-I) is embedded. HDL is key in the transportation of cholesterol in the body and removes cholesterol from macrophages in atherosclerotic plaques.[13,14] Due to the link between macrophage density and high-risk

*Joint corresponding authors

atherosclerotic plaque[15] or other inflammatory diseases,[16–18] the imaging of the expression of macrophages is an attractive goal.[15,19] We have previously reported HDL that has paramagnetic, gadolinium-labeled phospholipids incorporated and has been used for the T1-weighted MR imaging of macrophages in a mouse model of atherosclerosis.[20–22]

In an overlap of these two areas, new materials have recently been reported that incorporate both inorganic nanocrystals and natural nanoparticles and therefore possess novel combinations of properties. For example, viruses have been combined with quantum dots and carbon nanotubes to create covalently bound networks,[23] while Srivastava et al. have formed aggregates of ferritin and iron-platinum alloy nanoparticles that possess unusual magnetic properties.[24]

In the current study we use HDL to create such endogenous nanoparticle-inorganic material composites. In addition to modifying the phospholipid coating of HDL to provide contrast for medical imaging, we theorized that the natural hydrophobic core could be altered for the same purpose. Nanocrystals, such as gold nanoparticles, iron oxides and quantum dots can be synthesized with hydrophobic capping ligands[10,25,26] and so we attempted to replace the hydrophobic core of HDL with inorganic nanocrystals to produce novel contrast agents for molecular imaging. We herein report the synthesis of such HDL with a gold, iron oxide or quantum dot core. Fluorescent and paramagnetic lipids were included in the phospholipid corona of the particles as appropriate so that all the nanocrystal HDL were at least MRI and fluorescence active and therefore multimodal (Figure 1A).[27]

To synthesize the nanocrystal core HDL, first a ten-fold excess of the relevant phospholipids and the hydrophobic nanoparticle were co-dissolved in a 9:1 chloroform:methanol solvent mixture. For example, in the case of the gold nanoparticle three phospholipids were used. These were an ordinary phospholipid (MHPC), a gadolinium labeled phospholipid (Gd-DTPA-DMPE) and a rhodamine labeled phospholipid (Rhod-DMPE) and were added in a 50:50:1 mass ratio. The structures of these phospholipids are displayed in Figure 1B, their full names are given in the Supporting Information. This solution was added dropwise to hot (80°C), stirred, deionized water (Figure 1B). This process caused the immediate evaporation of the organic solvents resulting in the swift formation of micellar structures with inorganic nanoparticles lodged in the core of some of these phospholipid aggregates. Careful choice of lipids and methodical adjustment of the experimental conditions produced dispersions of a mixture of inorganic nanoparticles individually encapsulated in the core of phospholipid micelles and phospholipid micelles without nanocrystals. The buffer was changed to PBS and apoA-I, the primary protein constituent of HDL, was added in a 1:2.5 mass ratio to the phospholipids. Incubation of this mixture overnight allowed the incorporation of apoA-I into the lipidic corona,[28] forming HDL-like particles.

Exploiting the high density of the inorganic nanoparticles, we isolated the nanocrystal HDL by using a modification of Havel's ultracentrifugation lipoprotein separation method[29] where 30% KBr solution was used. Purified nanocrystal HDL was prepared for biological application by changing the buffer to PBS, which was subsequently followed by filtering and concentrating the solution. Henceforth, the different nanocrystal HDL are referred to as Au-HDL, FeO-HDL and QD-HDL. Control particles were synthesized according to analogous methods except a pegylated phospholipid, DSPE-PEG, was used in place of MHPC and apoA-I was not added, thereby creating non-specific particles, with equally good pharmacokinetics, but no inherent affinity for macrophages.[30,31] These particles are referred to as Au-PEG, FeO-PEG and QD-PEG.

The ionic relaxivities r1 and r2, indicate the potency of an MRI contrast agent to generate contrast. We determined r1 and r2 for the different particles at 60 MHz and 40 °C (Table 1).

The agents we propose for T1 weighted imaging, Au-HDL and QD-HDL, have r1s of 13.1 and 11.7, and a r2/r1 ratios of 1.3, which are typical of T1 contrast agents.[32] For the superparamagnetic FeO-HDL, the r2/r1 ratio of 10.6 is high, which makes this agent highly suitable for T2 or T2* weighted MR imaging.

Comparison of phosphorous and gadolinium analyses revealed that the ratio of Gd-DTPA-DMPE to MHPC for Au-HDL and QD-HDL was the same as the input reaction ratio, i.e. 1:1. The quantity of phospholipids was very similar to the amount required to coat the number of nanoparticles in the solution, indicating that the removal of the 'empty' particles had been successful. Protein analysis revealed that the incorporation of apoA-I into the particles had been successful (Table 1).

Negative stain TEM indicated that only HDL or PEG-coated particles with one nanocrystal core remained as depicted for the iron oxide particles in Figure 1C and D and for the gold and quantum dots in the Supporting Information (Figure S1). Analysis of the TEM images revealed that the size of the inorganic cores for the gold, iron oxides and quantum dots had mean diameters of 5.6, 6.3 and 6.6 nm, respectively, while their total particle diameters, including the phospholipid corona, were 9.7, 11.9 and 12.0 nm, in line with increases in the core size. Similar diameters were observed by gel electrophoresis and dynamic light scattering measurements and so the Au-HDL FeO-HDL and the QD-HDL are within the normal size range of HDL (7–13 nm)[33]. Taking together the particle size, phospholipid coating, apoA-I content and hydrophobic core, the nanocrystal HDL can be considered very similar to native HDL.

The diameters derived from the TEM images for the PEG-coated particles are substantially smaller than those found via DLS measurements. This is explained by the fact that the phosphotungstate stain used in the TEM imaging penetrates the PEG chains and thus they are not visible using that technique.[34] As a result, the PEG-coating and thereby the total particle-size appears smaller in negative-staining TEM as compared to DLS.

The absorbance and emission spectra of the QD-HDL are displayed in Figure 1E. The particles absorb light strongly below 550 nm and emit the absorbed light in a narrow band, typical for QDs, centered at 623 nm. In Figure 1F two photographs are displayed where the appearance of the QD-HDL solution under ambient light and UV light clearly indicate that the fluorescence can be observed by the naked eye.

As examples of the contrast-producing properties of nanocrystal HDL, we have included CT, fluorescence and MR images of phantoms of Au-HDL suspensions in Figure 1G-I (note: the solutions are of different concentration ranges in the different images). It is clear that Au-HDL provides contrast for each imaging modality, brightening the image in each case with increasing concentration. From the CT images we found the attenuation to be linear up to about 2500 HU or 400 mM Au and were able to establish the attenuation of the particles to be 6.4 HU/mM Au at 110 keV. In comparison, the attenuation of Omnipaque® (Nycomed Imaging AS, Oslo, Norway), a clinically-used, radiographic, iodine-based contrast agent, was found to be 4.3 HU/mM I (see Figure S3, Supporting Information). Our gold-based agent is therefore superior, as it attenuates X-rays at a rate 1.5 times that of Omnipaque. This higher rate is in agreement with a study by Kim et al. who have compared gold nanoparticle-based and iodine-based CT contrast agents.[35] The attenuation window in Figure 1H is set to display the contrast produced by this range of concentrations. However, a variety of attenuation windows may be used, including 0 to 200 HU where there is excellent contrast between saline and 4 mg Au/ml (1.3 nM of nanoparticles) Au-HDL, as displayed in Figure S2 in the supporting information. Furthermore, 30 HU is considered sufficient to distinguish between tissues and corresponds to 5 mM Au.[36]

Previous HDL-based contrast agents have been shown to be macrophage specific,[20] therefore *in vitro* uptake experiments were undertaken with a J774A.1 mouse macrophage cell line, cultured in DMEM supplemented with 10% FBS and 1% streptomycin/penicillin. Cells were incubated with the nanocrystal-HDL, relevant control contrast agents or with media only for 0.5, 1, 2, 4, 7 and 12 hours before being harvested, washed, and preserved as pellets for the imaging experiments. In the case of Au-HDL, the control agents were Au-PEG and Omnipaque and each was added to the wells such that the concentration of Au/I was 0.5 mg/ml. Preferential uptake of Au-HDL over Au-PEG was established via confocal microscopy of macrophage cells incubated for 2 hours with the agents (Figure 2A, B), where the red signal corresponds to rhodamine incorporated in the lipid coating of the particles. In Figure 2C TEM images indicate that Au-HDL binds to the cell surface before being internalized into lysosomes.

The cell pellets were imaged on a clinical CT scanner (Siemens Somatom Emotion 6, Malvern, PA) at 110 keV, as shown in Figure 2D (note: the top 4/5 of the material in each image is the preservative paraformaldehyde, the area at the bottom tip of the image is the cell pellet). The cell pellets incubated with Au-HDL appear bright, whereas the pellets incubated with other agents are indistinguishable from the paraformaldehyde solution. The increases in attenuation of each cell pellet (compared to the cells incubated with media) as a function of incubation time are presented in Figure 2E. In these attenuation ranges the absorption of X-rays is directly proportional to the concentration of contrast agent taken up by the cells. It can be seen that the Au-HDL is taken up very swiftly initially but at a slower rate thereafter, consistent with saturation of a receptor-mediated process. Receptor mediated uptake is likely, as HDL binds to the SR-B1[37] and ABCA-I[38] macrophage receptors.

Lastly, T1-weighted MR imaging was performed on the cell pellets using a 9.4 T system (Bruker, Billerica, MA). In Figure 2F the image for the 4 hour-incubated cells is displayed. As evident from this image, the cells incubated with the Au-HDL appear much brighter than the cells incubated with the Au-PEG or with media only, which revealed uptake as increasing concentrations of gadolinium ions produces image brightening in this form of MRI.[39]

Similar to Au-HDL, macrophage cells took up FeO-HDL more pronouncedly than FeO-PEG, as observed by confocal microscopy, TEM and MRI (Figure 3). Incubations were carried out at using a concentration of 4 μg Fe/ml. T2-weighted MR imaging of pellets of these cells showed a typical darkening of the cell pellets incubated with FeO-HDL, while the cells incubated with media only or FeO-PEG appear bright. An example image is shown in Figure 3D. This indicates preferential uptake of FeO-HDL, as iron particles produce darkening on T2-weighted MR images due to signal dephasing.

Cells incubated with QD-HDL (using a 0.02 mM Gd dose) had a high level of fluorescence as compared with cells incubated with QD-PEG, as shown in Figure 4A and B. As for Au-HDL, the cells incubated with QD-HDL appeared bright on T1-weighted MR images as compared to cells incubated with QD-PEG or media only (Figure 4C). TEM images also revealed uptake of QD-HDL by the cells, as depicted in Figure 4D. Fluorescence imaging corroborated the difference in uptake between QD-HDL and QD-PEG. This can be appreciated visually by the comparison of photos of the cell pellets taken in ambient light (Figure 4E) and under UV light illumination (Figure 4F). The effect was quantified using an IVIS fluorescence imaging system (Xenogen, Alameda, CA), the results of which are displayed in Figure 4G and clearly demonstrate the greater specificity of the QD-HDL for macrophages.

With the in vitro experiments we have shown the multimodal character of the nanocrystal core-HDL platform by imaging the cells incubated with these agents using confocal microscopy, MRI, CT, fluorescence imaging and TEM. For all the different cores the nanocrystal-HDL is

taken up at a much greater extent than the PEG-coated equivalent particle, demonstrating the high affinity for macrophages.

As a proof-of-principle study of the *in vivo* imaging efficacy of nanocrystal-core HDL, we injected the different nanocrystal-HDL or nanocrystal-PEG particles into apoE KO mice. These mice, after being on a high-cholesterol diet for 10 months, are an established model of atherosclerosis.[40] Twenty mice were included in this study, three for each agent and two as controls. The abdominal aorta of these mice were imaged pre- and 24 hours post intravenous administration of the different agents using a 9.4 T, dedicated small animal MRI scanner. The gold and quantum dot based agents were injected at a 50 μmol Gd/kg dose (equivalent to ca. 500mg Au/kg or 57 nmol QD per mouse), while the iron oxide agents were injected at a 30 mg Fe/kg dose. Typical results of such imaging are displayed in Figure 5A-F. There is a clear increase in the signal intensity in the aortic wall in the post-scans for the Au-HDL and QD-HDL and a clear decrease for the FeO-HDL, which are the expected effects for T1 (Au-HDL and QD-HDL) and T2/T2* (FeO-HDL) MRI contrast agents. Analysis of the normalized enhancement ratio of the post-scan compared to the pre-scan revealed a signal enhancement (given as the mean ± the standard deviation) of 139 ± 25% and 69 ± 23% for Au-HDL and QD-HDL, respectively. As is typical for T2/T2* agents, a signal drop of 53 ± 11% was observed for FeO-HDL. Perl's (iron) staining of aorta sections of mice injected with FeO-HDL further proved that these particles had lodged within the wall (Figure S4, Supporting Information). Although the QD-HDL gave a lower average enhancement than the gold, this was not found to be a statistically significant difference. The corresponding values for Au-PEG, QD-PEG and FeO-PEG were 35 ± 11%, 20 ± 13% and 6 ± 8%, respectively, none of which were a significantly different from the pre-contrast situations.

Furthermore, two types of fluorescence techniques were used to confirm the localization and to identify the specificity of the particles in the aorta. Confocal microscopy was performed on sections of aortas excised from the mice 24 hours post-injection. The sections were stained for macrophages (green) and for nuclei (blue), while the signal from the agent was displayed in red; the results are presented in Figure 5G-I. Channel-split images of the confocal microscopy are shown in Figures S5–7 in the Supporting Information. Areas of co-localization between the agent and macrophages appear as orange/yellow and so it can be seen that each HDL-coated particle was associated with macrophages. Alternatively, the excised aortas of the mice were imaged using a Maestro™ fluorescence imaging system (CRI Inc, Woburn, MA) that allows the fluorescence signal from the injected fluorophores to be isolated. While it may be advantageous to use NIR fluorophores as tissue autofluorescence is low in that wavelength range, we found this spectral unmixing function to satisfactorily remove autofluorescence. An example of the results of this imaging for the QD-HDL and its controls is shown in Figure 5J (further examples for Au-HDL and FeO-HDL are shown in Figures S8 and S9 Supporting Information). As can be seen, this imaging confirms the results found with MRI: the nanocrystal-HDL is heavily taken up into the aorta wall, to a much greater extent than QD-PEG control particles.

In addition, the aortas of the mice injected with gold particles and the aortas of two uninjected (control) mice were excised and imaged using a small animal CT scanner operating at 60 keV (microCAT II, ImTek Inc). As can be seen in Figure 5K, the aortas of mice injected with Au-HDL exhibit bright (i.e. highly attenuating) areas. Such bright spots were not observed in the aortas of control or Au-PEG injected mice. The mean signal to noise ratio (SNR) found in the bright areas of Au-HDL aortas was 23.5 ± 3.9, while the values of Au-PEG and control aortas were very similar to one another; 15.7 ± 5.2 and 14.7 ± 3.2, respectively. The SNR of the Au-HDL aortas was significantly higher than both the Au-PEG and control aortas, while the Au-PEG SNR was not significantly different from that of the control. The uptake of Au-HDL could also be distinguished by the naked eye due to the strong reddish hue of the particles (Figure

S10, Supporting Information). In the CT image of the aorta (Figure 5K) two hotspots originating form AU-HDL accumulation can be identified. This observation was in excellent agreement with the distribution of fluorescence of the same aorta displayed in Figure S9 (the aorta lowest in the image) of the Supporting Information. Taken together these results indicate that nanocrystal HDL can be very successfully applied for molecular imaging of atherosclerosis.

In this current study, we have introduced a new platform for molecular imaging: nanocrystal core HDL. The composition of this novel amalgamation of inorganic and natural nanoparticles can be altered to provide contrast for multiple imaging modalities, which we have demonstrated by applying the nanocrystal-HDL to cells *in vitro* and atherosclerotic mice *in vivo*.

As well as the compositions discussed in detail in this paper, we have synthesized nanocrystal HDL where the phospholipid coating is composed of different combinations of phospholipids with, for example, variations of acyl chain length and headgroup composition, similarly to variations observed in native lipoproteins. We have also used apoA-I mimicking peptides such as 37pA,[41] in place of the natural protein. This indicates that there is a substantial degree of flexibility in the lipid coatings that may be used with our synthesis procedure.

Due to the high sensitivity of fluorescence imaging it can be seen that there is extensive contrast throughout the aortas treated with QD-HDL. CT, however, has a much lower sensitivity and hence there are only a few bright spots in the aorta treated with Au-HDL. These bright spots correspond to areas of plaque with high macrophage content, namely the aortic arch and near the renal arteries.[42] Atherosclerotic plaques of high macrophage content have been identified as at risk of rupture and may lead to a heart attack.[15] Thus Au-HDL combined with CT imaging may have attractions for identifying these high risk plaques.

As control nanoparticles we considered the possibility of using nanocrystals coated with the same phospholipids, similar to the HDL particles, but without the inclusion of apoA-I (nanocrystal micelles). However, we found that PEG-coated nanocrystals had two significant advantages over nanocrystal micelles. Firstly, the latter control particles were unstable over time, aggregating and precipitating, particularly at low concentrations, which was not the case for PEG-coated nanocrystals. The reason for this discrepancy (as compared to nanoparticles that had apoA-I included) is because apoA-I lowers the surface pressure of the lipid coating of the particles and therefore stabilizes the nanoparticle assemblies. Indeed the nanocrystal HDL was found to be stable over extended periods (three months) and did not aggregate or precipitate. Secondly, one of the advantages of basing contrast agents on endogenous nanoparticles is that they evade clearance from the circulation and we felt that a suitable control particle should do that as well, motivating us to use PEG-coated particles which exhibit enhanced blood half-lives.[30,31]

Nanocrystal core HDL could potentially be used to investigate the metabolism of HDL *in vivo*, in particular how cells interact with this lipoprotein. The inherent solid character of the core enables a precise tuning of the size of the particle, which may be employed to investigate size dependent HDL-cell interactions. Additionally, since the core may be labeled differently from the HDL corona, the dissociation of the particle may be investigated.

In the current study, we have imaged macrophage expression in atherosclerosis. Imaging this cell type can also be useful in a variety of inflammatory diseases such as rheumatoid arthritis, liver disease and cancer.[16–18] As a further extension, this imaging platform may be re-routed to other disease markers by conjugating the appropriate targeting ligand to the apolipoprotein component.[12] In the field of targeted molecular imaging with nanoparticles[43] a variety of markers have been explored, including VCAM-1,[44,45] e-selectin[46,47] or $\alpha_v\beta_3$-integrin[48–50] for improved visualization of atherosclerosis and cancer related processes. We intend to

thoroughly investigate the *in vivo* properties of this novel contrast agent platform in different disease models, employing clinical scanners in the process.

To conclude, we have successfully prepared multimodal nanocrystal HDL for molecular imaging. We have established that these particles are in the size range of native HDL, to contain apoA-I, to have a phospholipid coating and a hydrophobic core. Thus these nanoparticles closely mimic endogenous HDL. In addition we have demonstrated the avid uptake of the nanocrystal HDL by macrophages *in vitro* using confocal microscopy, TEM, CT, T1-weighted MRI, T2-weighted MRI and fluorescence imaging. The *in vivo* applicability of the nanocrystal HDL for multimodality imaging of atherosclerosis was demonstrated. Also this is one of the first reports of a targeted contrast agent for CT.[51] While in this study we focused on atherosclerosis, we envisage that this nanoparticle platform could be used to detect molecular and cellular targets in a wide range of pathologies using multiple imaging modalities.

Supplementary Material

Refer to Web version on PubMed Central for supplementary material.

Acknowledgements

Partial support was provided by: NIH/NHLBI R01 HL71021, NIH/NHLBI R01 HL78667 (ZAF). We thank CSL Ltd, Parkville, Australia for their kind gift of apolipoprotein A-I. We gratefully acknowledge the assistance of the CT technicians of Mount Sinai Hospital in acquiring CT images. In addition, we would like to acknowledge the invaluable help and assistance of Heather Bell of the Mount Sinai Pathology EM core. Confocal microscopy was performed at the MSSM–Microscopy Shared Resource Facility and supported by NIH–National Cancer Institute Grant 5R24 CA095823-04, National Science Foundation Grant DBI-9724504, and NIH Grant 1 S10 RR0 9145-01. We thank Dr. Felix R. Wolf and Ms Valerie Longo of Cornell University/Memorial Sloan-Kettering Cancer Center (MSKCC) for their help with the experiments performed there. Technical services provided by the MSKCC Small-Animal Imaging Core Facility, supported in part by NIH Small-Animal Imaging Research Program (SAIRP) Grant No R24 CA83084 and NIH Center Grant No P30 CA08748, are gratefully acknowledged.

References

1. Mulder WJM, Cormode DP, Hak S, Lobatto ME, Silvera S, Fayad ZA. Nat Clin Pract Cardiovasc Med 2008;5:S103–S111. [PubMed: 18641599]
2. Kim D, Park S, Lee JH, Jeong YY, Jon S. J Am Chem Soc 2007;129:7661–7665. [PubMed: 17530850]
3. El-Sayed IH, Huang X, El-Sayed MA. Nano Lett 2005;5:829–834. [PubMed: 15884879]
4. Jaffer FA, Libby P, Weissleder R. Circulation 2007;116:1052–1061. [PubMed: 17724271]
5. de Vries IJM, Lesterhuis WJ, Barentsz JO, Verdijk P, van Krieken JH, Boerman OC, Oyen WJG, Bonenkamp JJ, Boezeman JB, Adema GJ, Bulte JWM, Scheenen TWJ, Punt CJA, Heerschap A, Figdor CG. Nature Biotechnology 2005;23:1407–1413.
6. Bulte JWM, Kraitchman DL. NMR in Biomedicine 2004;17:484–499. [PubMed: 15526347]
7. Wickline SA, Neubauer AM, Winter P, Caruthers S, Lanza G. Arterioscler Thromb Vasc Biol 2006;26:435–441. [PubMed: 16373609]
8. Medintz IL, Uyeda HT, Goldman ER, Mattoussi H. Nat Mater 2005;4:435–446. [PubMed: 15928695]
9. Kobayashi H, Hama Y, Koyama Y, Barrett T, Regino CAS, Urano Y, Choyke PL. Nano Lett 2007;7:1711–1716. [PubMed: 17530812]
10. Michalet X, Pinaud FF, Bentolila LA, Tsay JM, Doose S, Li JJ, Sundaresan G, Wu AM, Gambhir SS, Weiss S. Science 2005;307:538–544. [PubMed: 15681376]
11. Manchester M, Singh P. Adv Drug Deliv Rev 2006;58:1505–1522. [PubMed: 17118484]
12. Zheng G, Chen J, Li H, Glickson JD. Proc Natl Acad Sci USA 2005;102:17757–17762. [PubMed: 16306263]
13. Lusis AJ. Nature 2000;407:233–241. [PubMed: 11001066]
14. Linsel-Nitschke P, Tall AR. Nat Rev Drug Discov 2005;4:193–205. [PubMed: 15738977]

15. Naghavi M, Libby P, Falk E, Casscells SW, Litovsky S, Rumberger J, Badimon JJ, Stefanadis C, Moreno P, Pasterkamp G, Fayad Z, Stone PH, Waxman S, Raggi P, Madjid M, Zarrabi A, Burke A, Yuan C, Fitzgerald PJ, Siscovick DS, de Korte CL, Aikawa M, Airaksinen KEJ, Assmann G, Becker CR, Chesebro JH, Farb A, Galis ZS, Jackson C, Jang IK, Koenig W, Lodder RA, March K, Demirovic J, Navab M, Priori SG, Rekhter MD, Bahr R, Grundy SM, Mehran R, Colombo A, Boerwinkle E, Ballantyne C, Insull W, Schwartz RS, Vogel R, Serruys PW, Hansson GK, Faxon DP, Kaul S, Drexler H, Greenland P, Muller JE, Virmani R, Ridker PM, Zipes DP, Shah PK, Willerson JT. Circulation 2003;108:1664–1672. [PubMed: 14530185]
16. Morand EF, Leech M, Bernhagen J. Nat Rev Drug Discov 2006;5:399–411. [PubMed: 16628200]
17. Shi L, Kishore R, McMullen MR, Nagy LE. J Biol Chem 2002;277:14777–14785. [PubMed: 11856733]
18. van der Bij GJ, Oosterling SJ, Meijer S, Beelen RHJ, van Egmond M. Cellular Oncology 2005;27:203–213. [PubMed: 16308469]
19. Sanz J, Fayad ZA. Nature 2008;451:953–957. [PubMed: 18288186]
20. Frias JC, Ma Y, Williams KJ, Fayad ZA, Fisher EA. Nano Lett 2006;6:2220–2224. [PubMed: 17034087]
21. Cormode DP, Mulder WJM, Fisher EA, Fayad ZA. Future Lipidol 2007;2:587–590.
22. Cormode DP, Briley-Saebo KC, Mulder WJM, Aguinaldo JGS, Barazza A, Ma Y, Fisher EA, Fayad ZA. Small 2008;4:1437–1444. [PubMed: 18712752]
23. Portney NG, Singh K, Chaudhary S, Destito G, Schneemann A, Manchester M, Ozkan M. Langmuir 2005;21:2098–2103. [PubMed: 15751992]
24. Srivastava S, Samanta B, Jordan BJ, Hong R, Xiao Q, Tuominen MT, Rotello VM. J Am Chem Soc 2007;129:11776–11780. [PubMed: 17803305]
25. Brust M, Walker M, Bethell D, Schiffrin DJ, Whyman R. Chem Commun 1994:801–802.
26. Gupta AK, Gupta M. Biomaterials 2005;26:3995–4021. [PubMed: 15626447]
27. Frullano L, Meade TJ. J Biol Inorg Chem 2007;12:939–949. [PubMed: 17659368]
28. Jonas A. Method Enzymol 1986;128:553–582.
29. Havel RJ, Eder HA, Bragdon JH. J Clin Invest 1955;34:1345–1353. [PubMed: 13252080]
30. Klibanov AL, Maruyama K, Torchilin VP, Huang L. FEBS Lett 1990;268:235–238. [PubMed: 2384160]
31. Allen TM, Hansen C, Martin F, Redemann C, Yau-Young A. Biochimica et Biophysica Acta (BBA) - Biomembranes 1991;1066:29–36.
32. Mulder WJM, Koole R, Brandwijk RJ, Storm G, Chin PTK, Strijkers GJ, Donega CD, Nicolay K, Griffioen AW. Nano Lett 2006;6:1–6. [PubMed: 16402777]
33. Nichols AV, Krauss RM, Musliner TA. Method Enzymol 1986;128:417–431.
34. Huang X, Bronstein LM, Retrum J, Dufort C, Tsvetkova I, Aniagyei S, Stein B, Stucky G, McKenna B, Rennes N, Baxter D, Kao CC, Dragnea B. Nano Lett 2007;7:2407–2416. [PubMed: 17630812]
35. Kim D, Park S, Lee JH, Jeong YY, Jon S. J Am Chem Soc 2007;129:12585–12585.
36. Krause W. Adv Drug Deliv Rev 1999;37:159–173. [PubMed: 10837733]
37. Acton S, Rigotti A, Landschulz KT, Xu S, Hobbs HH, Kriegert M. Science 1996;271:518–520. [PubMed: 8560269]
38. Vedhachalam C, Ghering AB, Davidson WS, Lund-Katz S, Rothblat GH, Phillips MC. Arterioscler Thromb Vasc Biol 2007;27:1603–1609. [PubMed: 17478755]
39. Bottrill M, Kwok L, Long NJ. Chem Soc Rev 2006;35:557–571. [PubMed: 16729149]
40. Piedrahita JA, Zhang SH, Hagaman JR, Oliver PM, Maeda N. Proc Nat Acad Sci USA 1992;89:4471–4475. [PubMed: 1584779]
41. Navab M, Anantharamaiah GM, Reddy ST, Fogelman AM. Nat Clin Pract, Cardiovasc Med 2006;3:540–547. [PubMed: 16990839]
42. Nakashima Y, Plump AS, Raines EW, Breslow JL, Ross R. Arterioscler Thromb 1994;14:133–140. [PubMed: 8274468]
43. Artemov D. Journal of Cellular Biochemistry 2003;90:518–524. [PubMed: 14523986]

44. McAteer MA, Sibson NR, von zur Muhlen C, Schneider JE, Lowe AS, Warrick N, Channon KM, Anthony DC, Choudhury RP. Nat Med 2007;13:1253–1258. [PubMed: 17891147]
45. Nahrendorf M, Jaffer FA, Kelly KA, Sosnovik DE, Aikawa E, Libby P, Weissleder R. Circulation 2006;114:1504–1511. [PubMed: 17000904]
46. Mulder WJM, Strijkers GJ, Griffioen AW, vanBloois L, Molema G, Storm G, Koning GA, Nicolay K. Bioconjugate Chem 2004;15:799–806.
47. Kang HW, Torres D, Wald L, Weissleder R, Bogdanov AA. Lab Invest 2006;86:599–609. [PubMed: 16607378]
48. Winter PM, Caruthers SD, Kassner A, Harris TD, Chinen LK, Allen JS, Lacy EK, Zhang H, Robertson JD, Wickline SA, Lanza GM. Cancer Res 2003;63:5838–5843. [PubMed: 14522907]
49. Mulder WJM, Strijkers GJ, Habets JW, Bleeker EJW, Schaft DWJvd, Storm G, Koning GA, Griffioen AW, Nicolay K. FASEB J 2005;19:2008–2010. [PubMed: 16204353]
50. Sipkins DA, Cheresh DA, Kazemi MR, Nevin LM, Bednarski MD, Li KCP. Nat Med 1998;4:623–626. [PubMed: 9585240]
51. Hyafil F, Cornily JC, Feig JE, Gordon R, Vucic E, Amirbekian V, Fisher EA, Fuster V, Feldman LJ, Fayad ZA. Nat Med 2007;13:636–641. [PubMed: 17417649]

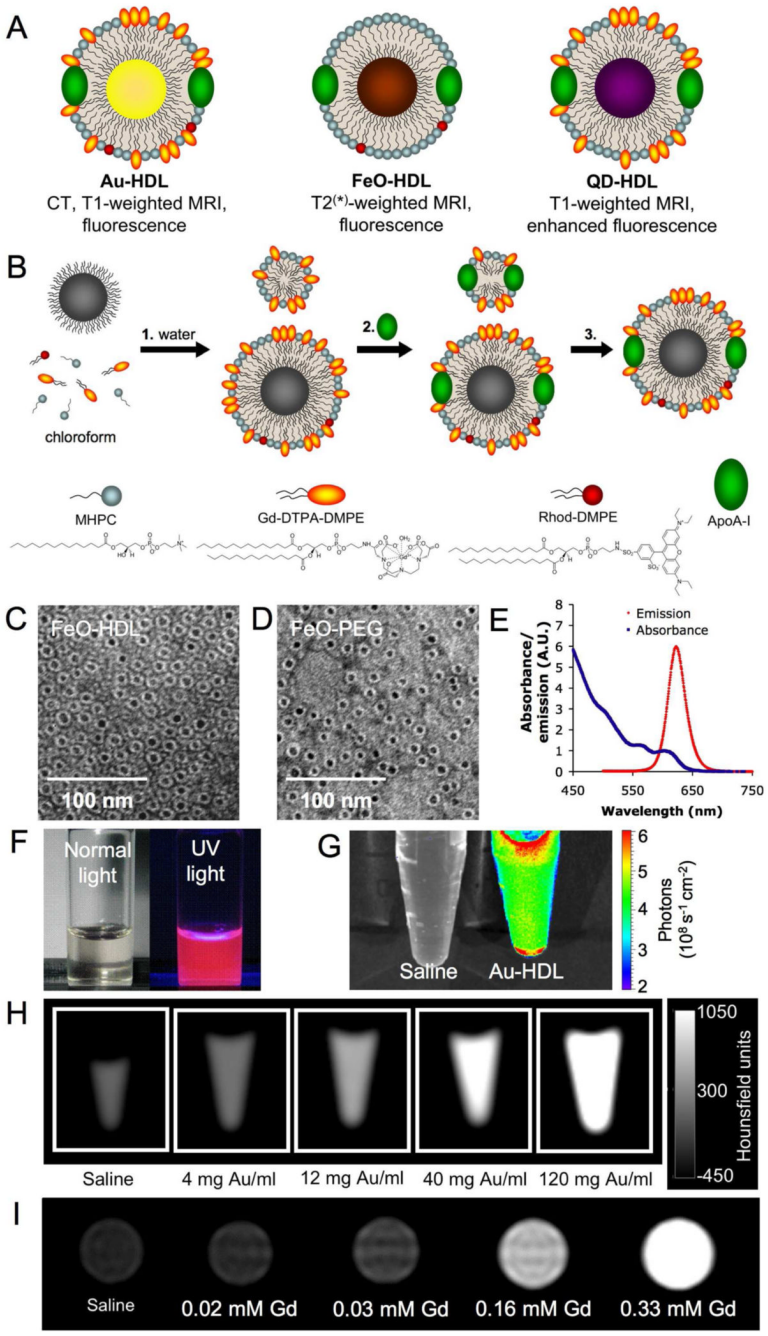

Figure 1. Nanocrystal core high density lipoprotein

A schematic depiction of the different agents in this study. **B** summary of the synthesis procedure of the agents where **1,** the phospholipids and nanocrystal in chloroform are added to water, **2,** apoA-I is added and **3,** the 'empty' particles are removed. **C** and **D** negative stain TEM images of FeO-HDL and FeO-PEG. **E** emission and absorption spectrum of the QD-HDL. **F** photograph of the QD-HDL in normal light (left) and under UV illumination (right). **G, H, I** phantoms of Au-HDL imaged using fluorescence, CT and MRI, respectively.

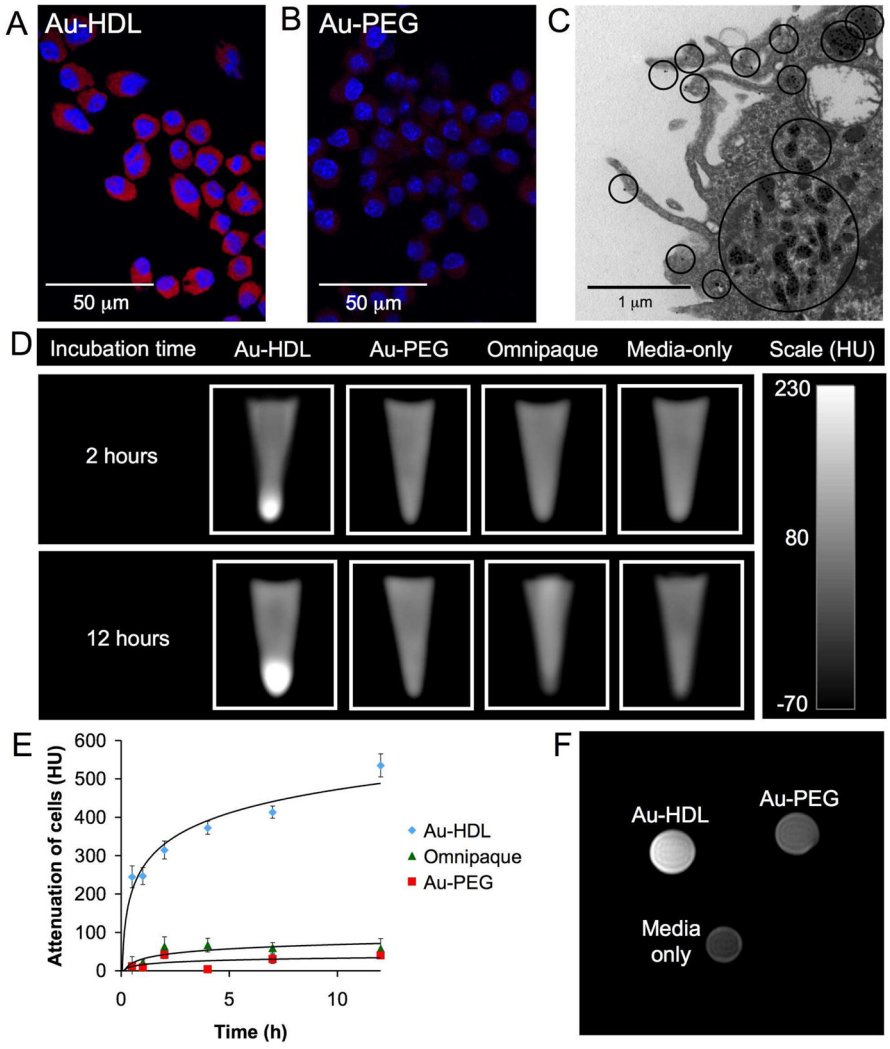

Figure 2. Uptake of Au-HDL by macrophage cells *in vitro*

A confocal microscopy of cells incubated for 2 hours with Au-HDL or **B** Au-PEG, which appear red (rhodamine) and the nuclei are stained with DAPI (blue). **C** TEM image where black circles indicate areas of particle uptake. **D** CT images of the different cell pellets. **E** graph of the increase in CT attenuation of the cell pellets compared to media only incubated cells vs. time of incubation. **F** T1-weighted MR image of cell pellets.

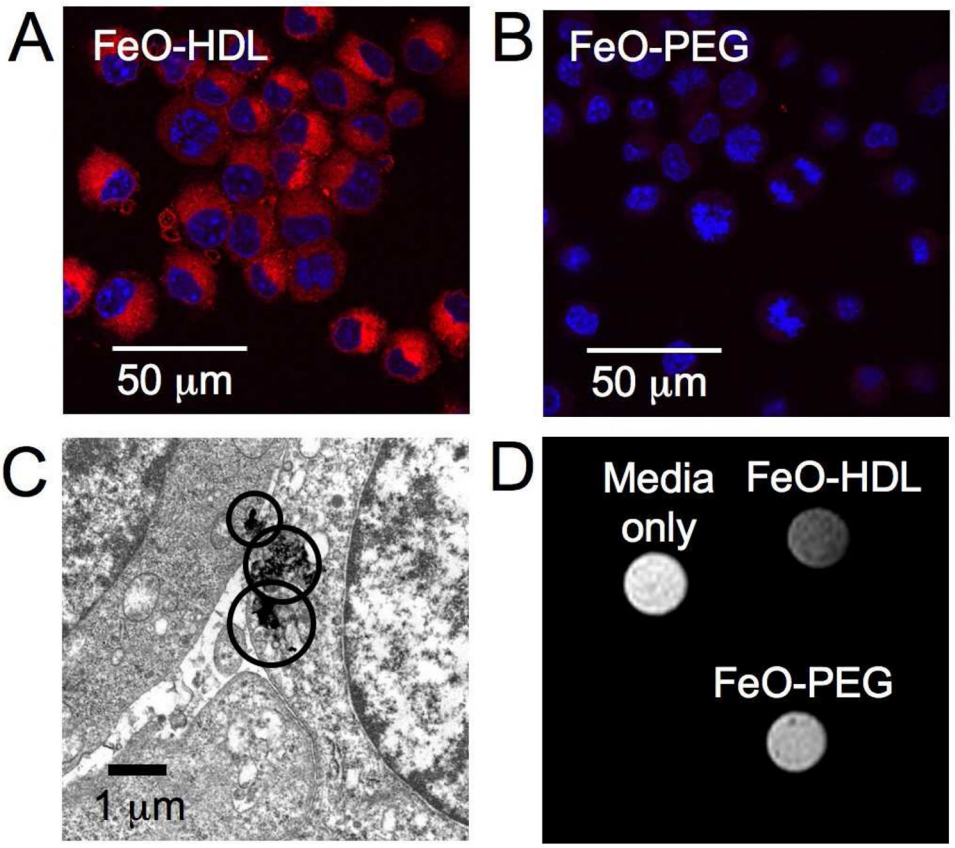

Figure 3. Uptake of FeO-HDL by macrophage cells *in vitro*

Confocal microscopy of cells incubated for 2 hours with **A** FeO-HDL and **B** FeO-PEG, where uptake is indicated by red (rhodamine) and the nuclei are stained with DAPI. **C** TEM of cells incubated with FeO-HDL, areas containing iron oxide are highlighted by circles. **D** T2-weighted MR image of cells incubated with FeO-HDL, FeO-PEG or media only for 4 hours.

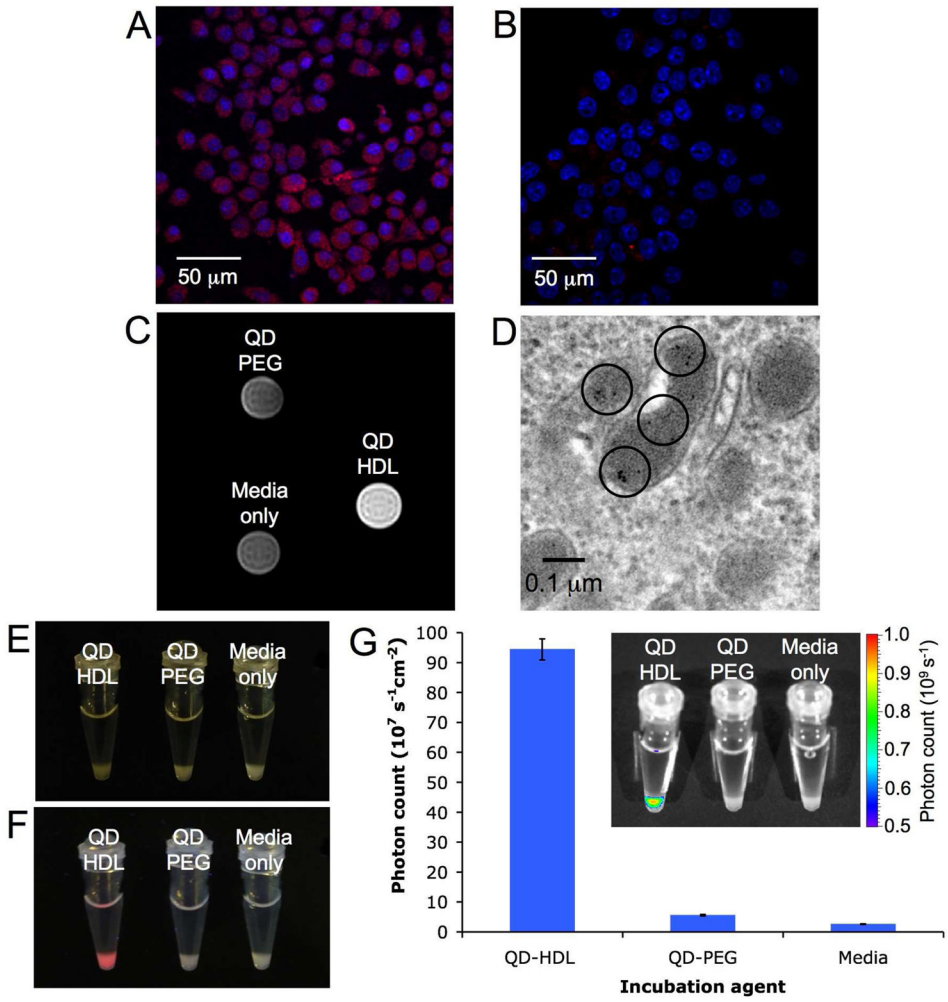

Figure 4. Uptake of QD-HDL by macrophage cells *in vitro*

Confocal microscopy of macrophage cells incubated for 2 hours, where **A** QD-HDL and **B** QD-PEG uptake is indicated by red and the nuclei are blue. **C** T1-weighted MR image of pellets of cells incubated for 4 hrs. **D** TEM image of QD-HDL uptake, QDs are highlighted with black rings. Photographs of the cell pellets taken under **E** ambient light and **F** UV irradiation. **G** chart of fluorescent intensity of the cell pellets, with a typical fluorescent image inset.

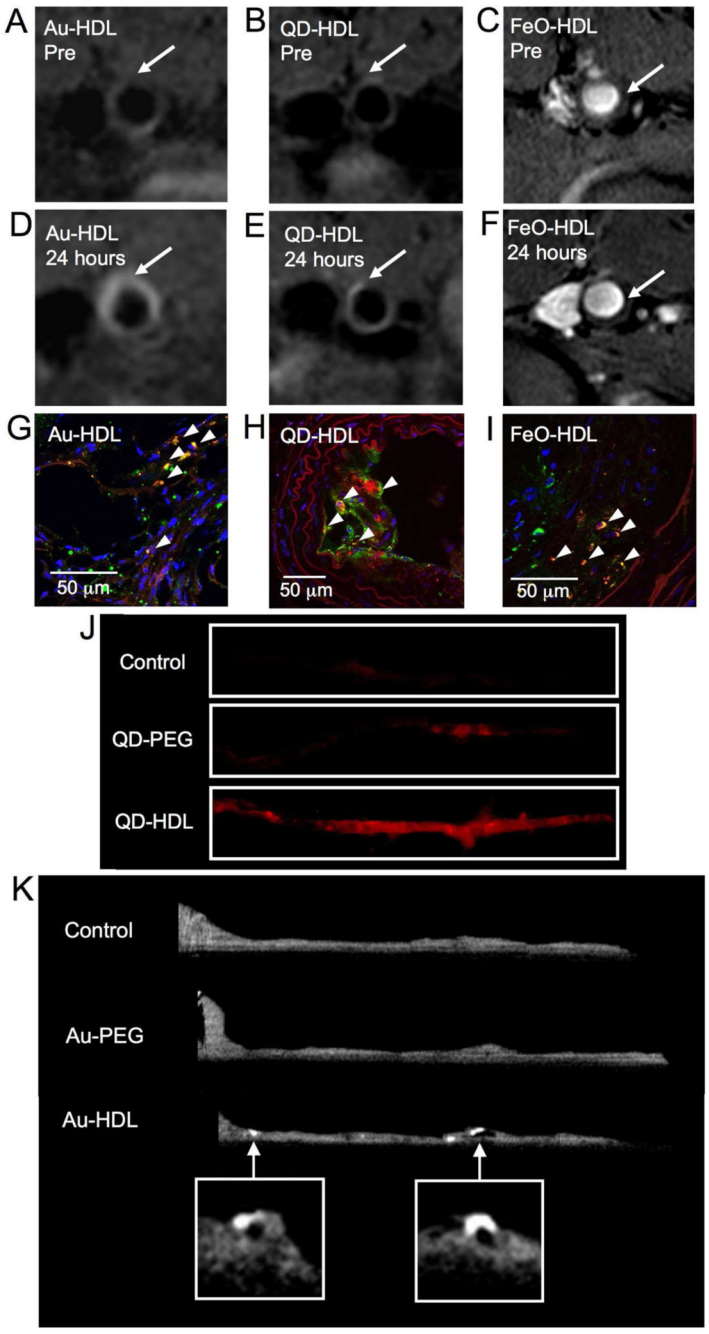

Figure 5. Multimodality imaging of atherosclerosis using nanocrystal high density lipoprotein

T1-weighted MR images of the aorta of apoE KO mice pre- (**A, B**) and 24 hours post-injection (**D, E**) with Au-HDL or QD-HDL. Arrows indicate areas enhanced in the post images. **C, F** T2*-weighted images of an apoE KO mouse pre- and 24 hours post-injection with FeO-HDL. **G, H, I** confocal microscopy images of aortic sections of mice injected with nanocrystal HDL. Red is nanocrystal HDL, macrophages are green and nuclei and blue. Yellow indicates co-localization of nanocrystal HDL with macrophages and is indicated by arrowheads. **J** fluorescence image of aortas of mice injected with QD-HDL, QD-PEG and saline. **K** *ex vivo* sagittal CT images of the aortas of mice injected with Au-HDL, Au-PEG and saline.

Table 1

Summary of the (physical) properties of nanocrystal HDL and PEG-coated control particles. Values are given as the mean ± the standard deviation.

Property (units)	Au-HDL	Au-PEG	FeO-HDL	FeO-PEG	QD-HDL	QD-PEG
r1 ($mM^{-1}s^{-1}$)	13.1 ± 0.3	12.2 ± 0.3	8.9 ± 0.3	11.6 ± 0.2	11.7 ± 0.4	13.0 ± 0.3
r2 ($mM^{-1}s^{-1}$)	16.8 ± 0.5	15.1 ± 0.6	94.2 ± 6.8	128.4 ± 7.2	14.8 ± 0.5	16.5 ± 0.7
Number of apoA-l molecules per particle	3.0	-	3.9	-	3.1	-
Core diameter (nm)	5.6 ± 1.0	5.8 ± 1.1	6.3 ± 1.0	6.5 ± 0.8	6.5 ± .08	5.9 ± 1.0
Diameter: TEM (nm)	9.7 ± 1.4	11.5 ± 1.5	11.9 ± 1.2	11.9 ± 1.4	12.9 ± 1.4	11.8 ± 1.6
Diameter: DLS (nm)	10.6 ± 1.8	19.2 ± 5.6	12.2 ± 1.6	20.7 ± 0.2	12.4 ± 2.3	18.3 ± 3.3
Diameter: gel electrophoresis (nm)	9.4 ± 1.0	-	11.2 ± 0.5	-	12.3 ± 1.1	-